Three Dimensional Elastic Plastic Analysis of a Semi-Elliptical Inner Surface Flaw by Finite Element Method

W. Brocks, H.-D. Noack, H. Veith

Bundesanstalt für Materialprüfung, Abt. 1, Fachreferat 1.01, Unter den Eichen 87, D-1000 Berlin 45, Germany

Summary

A three- dimensional elastic-plastic analysis for stresses and strains in a pressure vessel containing two semi-elliptical surface cracks was carried out by finite element (FE) method. Results for stress distribution, spreading of plastic zones and crack opening displacements are presented and discussed. The variation of the stress intensity factor along the crack front as gained from a linear elastic FE-analysis is compared with the result of the ASME Code procedure. First, the FE results are discussed according to the stress intensity concept using a plastic zone correction for small scale yielding. If the zone correction is done with plane stress approximations of IRWIN and DUGDALE, just slightly lower critical values are gained as by the FE-calculation. Introducing the same two dimensional models in the COD concept gives far too conservative estimations for the critical pressure for the plane stress solution, whereas the plane strain solution agrees quite well with the FE computations. All together, the COD concept is very sensitive to different methods of determining .

1. Introduction

The presence of flaws, mostly of semi-elliptical geometries, at the inner or outer surface of a pressure vessel or pipe increases the possibility of failure of those structures considerably due to stress concentrations around the flaws. Thus the fracture analysis of such structures is of utmost importance in assessing their structural integrety.

Various evaluations have been performed by analytical methods as well as by three dimensional elastic finite element computations to estimate the local stress intensity factors in plates with semi-elliptical surface flaws subjected to uniform tension or bending loads /1 - 4/ and in pressurized cylinders and vessels with inner or outer surface flaws /5 - 7/.

Many pressure vessels are operating at temperatures where major plastifications will occur before stable or unstable crack growth takes place. For these cases it has to be examined to what extent elastic concepts may still be used to determine local stresses as well as to apply material constants, and how to change to elastic-plastic concepts, if necessary. Such examinations have already been performed for a nozzle corner crack and the results of a three-dimensional elastic-plastic finite element (FE) analysis have been compared with two-dimensional approaches of elastic-plastic fracture mechanics /8/. It has been found that an elastic analysis with small scale yielding corrections under plane stress conditions was appropriate as a criterion to assess critical loads.

2. Structural Model and Finite Element Idealization

The pressure vessel is modelled by an open tube (fig. 1) with an inner radius r_i of 1400 mm, a wall thickness t of 140 mm and a total length of 3000 mm. Two approximately semi-elliptical cracks are located along opposite axial lines on the inner surface. Because of symmetry only one eighths of the structure has to be considered in the FE analysis. The mesh of this section has 420 elements and 1539 nodes. Calculations show that the considered length is sufficient for fading away the perturbations by the crack.

Fig. 2 shows the FE-model of the crack plane together with the evaluation paths of stresses, strains, and displacements. On the nodal paths 1-9 crack opening displacements and on the Gaussian paths 11-26 stress and strains are defined. The half length c of the crack is 240 mm and the depth a is 83 mm. So the characteristic geometry parameters of the problems are: $r_o/r_i = 1.10$, $a/t = 0.59$ and $a/c = 0.35$. As the crack configuration was adapted to experimental fatigue cracks in bent plates, it has no ideal semi-elliptical shape. Collapsed wedge-shaped singularity elements lie along the crack front. In addition, their midside nodes were shifted to the quarter position for the elastic analysis to establish the characteristic $1/\sqrt{r}$ singularity.

The calculations were performed with the FE-program AOINA using the elastic-plastic material model with the v. Mises yield condition and isotropic hardening. The equivalent uniaxial stress-strain curve based on compression tests of the German standard steel 20 MnMoNi 5 5 is approximated by a multilinear function. The yield strength σ_y is 480 N/mm³. Around the crack front the geometrically nonlinear updated Lagrangian (UL) analysis and in the remaining structure a merely material nonlinear (MNO) analysis was applied.

3. Results

The elastic FE-analysis which was done with a pressure of 100 bar gives the variation of K_I along the crack front (fig. 3). K_I was extrapolated from the stress field as well as from the displacement field. The K_I-curve shows two distinct local maxima. One lies at the penetration of the crack front with the vessel surface and the other in the centre of the crack front which is the point of maximum crack depth. The upper curve takes into account the pressure acting on the crack surface. The comparison of both curves demonstrates that loading of the crack surface increases K_I by a ΔK of about 250 $Nmm^{-3/2}$ at the maxima and of about 200 $Nmm^{-3/2}$ at the minimum. The global maximum (upper curve) of K_I = 2340 $Nmm^{-3/2}$ is in good agreement with the result using the procedure of the ASME Code /9/. The stress distribution in the ligament for purely elastic material can be seen in fig. 4 where two characteristic paths were chosen. Path 13 (φ = 11°) has a minimum K_I and path 26 (φ = 90°) a maximum K_I.

The rearrangement of stresses due to the plastification of the ligament is demonstrated in fig. 5 at a pressure of 400 bar for the paths 13 and 26. Caused by crack tip blunting the stresses have maxima at about 0.2 mm from the crack front in the ligament comparable to the result on notched pieces. Fig. 6 shows the variation of the normalized crack opening stress σ_{yy}/σ_y along the crack front in a distance of r = 0.2 mm for four different pressure levels. The calculated stresses oscillate numerically with increasing plastification, especially in the range of intense curvature of the crack front. Hence, the graphs were smoothed by taking the average value within each element. The change from the elastic to the plastic regime shifts the maximum of the crack opening stress from the crack centre φ = 90° to the margin (φ = 20°).

The spread of the plastic zone starts from the crack front (fig. 7). It reaches the outer surface at a pressure of about 400 bar if crack surface loading is taken into account. Weakened by the crack the wall above the crack will be subjected to increasing buckling in dependence on pressure as can be seen from fig. 8. The crack tip opening displacement (CTOD) δ_t in fig. 9 is nearly constant along the crack front at low pressure and forms a maximum in the centre of the crack front with rising pressure.

4. Discussion

The relevant quantities for failure assessment as for instance the stress intensity factor K_I, the radius r_y of the plastic zone in the ligament and the CTOD δ_t are varying along the crack front. In the following discussion, their values are taken in the middle of the crack front ($\varphi = 90°$) where K_I and δ_t have a maximum.

Using the stress intensity concept in the elastic-plastic regime a small scale yielding correction of the stress intensity factor K_I seems to be necessary. Taking the concept of a "notional" crack tip movement into the middle of the plastic zone as proposed by IRWIN, a corrected stress intensity

$$K^* = K_I \sqrt{(a + r_y)/a} \qquad (1)$$

can be calculated. Fig. 10 shows the increase of the radius r_y of the plastic zone in the ligament at the centre of the crack front in dependence on pressure p for the FE-calculation and various analytical approaches on 2D-models of IRWIN /10/ for plane stress and plane strain and of DUGDALE (plane stress) /11/. The corresponding equations are summarized in reference /12/. Although considerable differences in the spread of the plastic zone with increasing pressure are observed between the FE-results and the various approaches, fig. 11 demonstrates that there is practically no significant difference of the various K^*-curves due to the plastic zone correction up to about 200 bar. Therefore, a purely elastic analysis would be sufficient up to this pressure. For further increasing pressure, the elastic K_I-analysis as well as the K^*-curve using a plane strain zone correction yield to non-conservative estimations of the critical pressure whereas the plane stress approaches of IRWIN and DUGDALE are conservative that means the critical pressures are lower. Altogether, the differences between the various corrected K^*-curves as well as their deviation from the linear K_I-analysis are lower than those of the previously examined nozzle corner crack /12/. This is probably due to the greater ratio of crack length to ligament in the present problem because the remaining ligament limits to extension of the plastic zone.

There is dissent regarding the experimental methods of determining COD which sometimes results in strongly different findings. So it seems to be difficult to use the COD-concept as an assessment criterion in fracture mechanics. Nevertheless, for comparison with the results of the K-concept, a COD-analysis will be performed for the present problem because the crack opening displacement in dependence on pressure is also known from the FE-calculation. For comparison with the FE-curve, again δ_t-curves are determined from the 2D-models of IRWIN and DUGDALE together with the WESTERGAARD equations. As can be seen from fig. 12 there are already considerable deviations above a pressure of about 100 bar and accordingly the variance for the estimated critical pressures is high. The plane strain solution of IRWIN is conservative up to a pressure of about 350 bar in comparison to the FE-curve for δ_t. The results of IRWIN and DUGDALE for plane stress are evidently far too conservative which was already found in the analysis of the nozzle corner crack /12/.

References

/ 1 / IRWIN, G. R., "Crack-Extension Force for a Part-Through Crack in a Plate", J. Appl. Mech. Vol. 29 (1962), 651 - 654.

/ 2 / SMITH, F. W., SORENSEN, D. R., "The Semi-Elliptical Surface Crack - A Solution by the Alternating Method", Int. J. Fracture, Vol. 12 (1976), 47 - 57.

/ 3 / KOBAYASHI, A. S., "Crack Opening Displacement in a Surface Flawed Plate Subjected to Tension or Plate Bending", Proc. 2nd Int. Conf. Mech. Behaviour of Materials, Boston, Mass., USA, 1976.

/ 4 / NEWMAN, J. C., RAJU, I. S., "Analysis of Surface Cracks in Finite Plates Under Tension or Bending Loads", NASA Tech. Paper 1578, 1979.

/ 5 / ATLURI, S. N., KATHIRESAN, K., "3D-Analysis of Surface Flaws in Thick-Walled Reactor Pressure Vessels Using Displacement-Hybrid Finite Element Method", Nuclear Eng. and Design, Vol. 51 (1979), 163 - 176.

/ 6 / KOBAYASHI, A. S., EMERY, A. F., LOVE, W. J., JAIN, A., "Further Studies on Stress Intensity Factors of Semi-Elliptical Cracks in Pressurized Cylinders", 5th SMiRT, Paper G 4/1, 1977.

/ 7 / NEWMAN, J. C., RAJU, I. S., "Stress Analysis and Fracture of Surface Cracks in Cylindrical Pressure Vessels, 5th SMiRT, Paper G 7/3, 1979.

/ 8 / BROCKS, W., NOACK, D., VEITH, H., "Elastic Plastic Analysis of a Nozzle Corner Crack by Finite Element Method", 6th SMiRT, Paper G 3/6, 1980.

/ 9 / ASME Boiler and Pressure Vessel Code (1981) Section XI, Appendix A.

/ 10 / IRWIN, G. R., "Structural Aspects of Brittle Fracture", Appl. Mat. Research 3, (1964), 65 - 81.

/ 11 / DUGDALE, D. S., "Yielding of Steel Sheets Containing Slits", J. Mech. Phys. Solids 8 (1960), 100 - 104.

/ 12 / BROCKS, W., NOACK, D., VEITH, H., "Elastic-Plastic Analysis of a Nozzle Corner Crack by Finite Element Method", Int. J. Pres. Ves. and Piping, 10 (1982), 219 - 234.

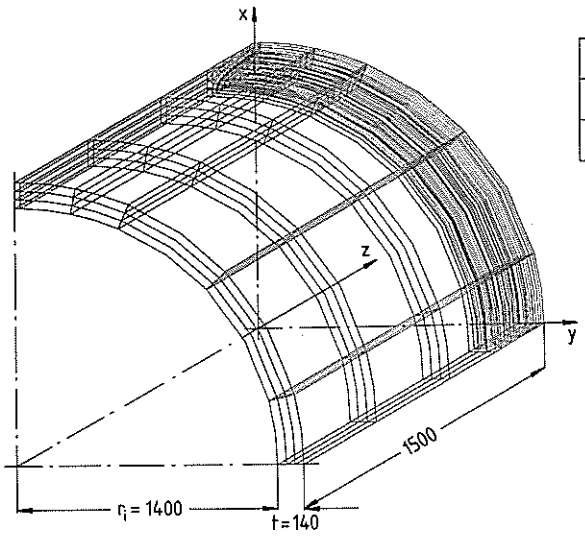

Fig. 1 - Finite element structure

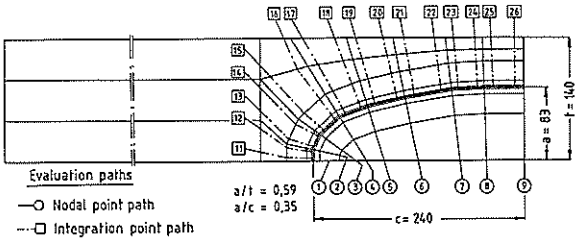

Fig. 2 - FE-model of the crack plane with the evaluation paths of stresses, strains and displacements

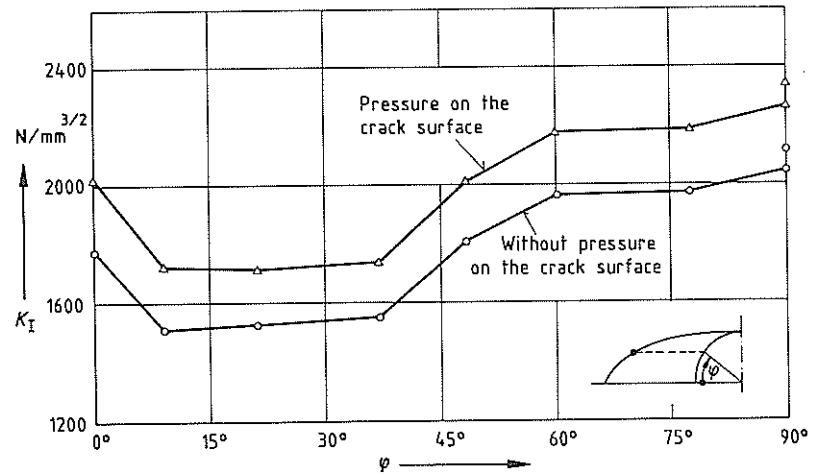

Fig. 3 - Stress intensity factor K_I along the crack front

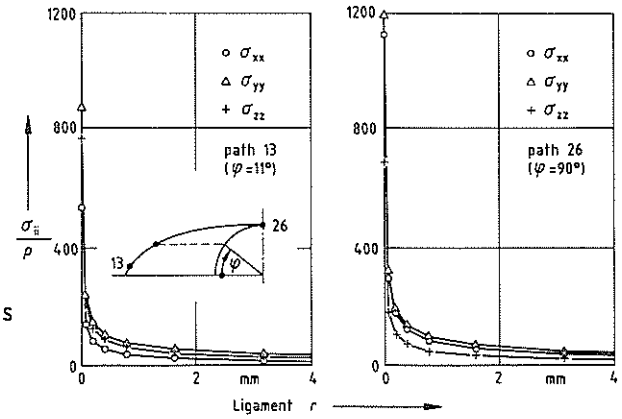

Fig. 4 - Normalized normal stresses σ_{ii}/p in the ligament along the paths 13 and 26 in the elastic range

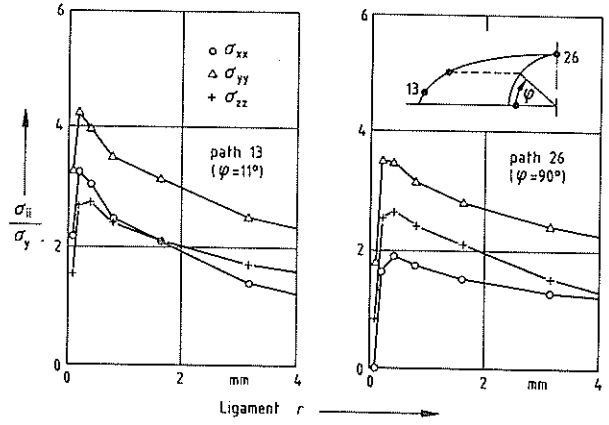

Fig. 5 - Normalized normal stresses σ_{ii}/σ_y in the ligament along the paths 13 and 26 in the plastic range at 400 bar

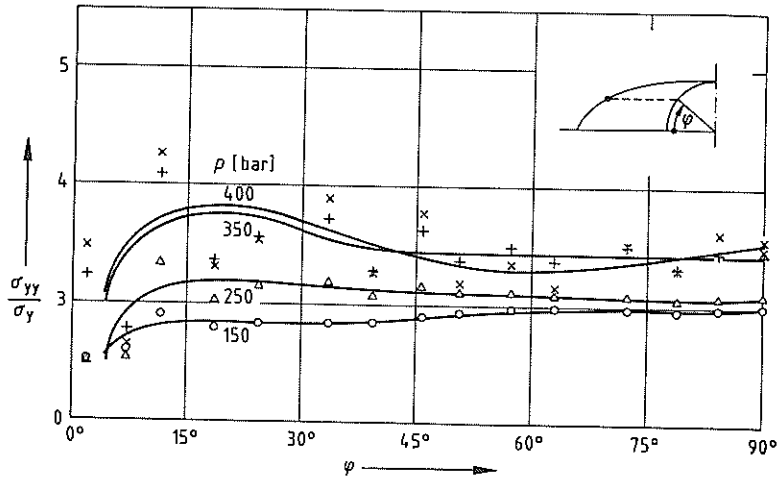

Fig. 6 - Normalized crack opening stress σ_{yy}/σ_y along the crack front at a distance of r = 0.2 mm for 150, 250, 350 and 400 bar

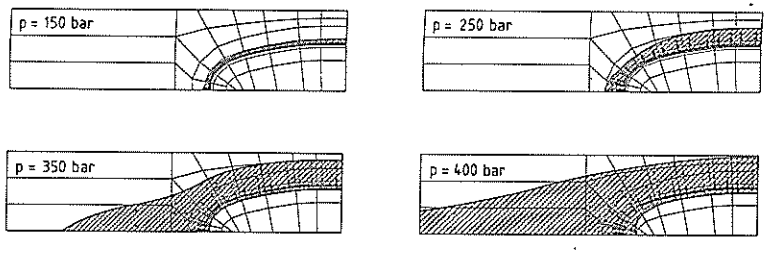

Fig. 7 - Spreading of the plastic zone through the ligament with increasing pressure

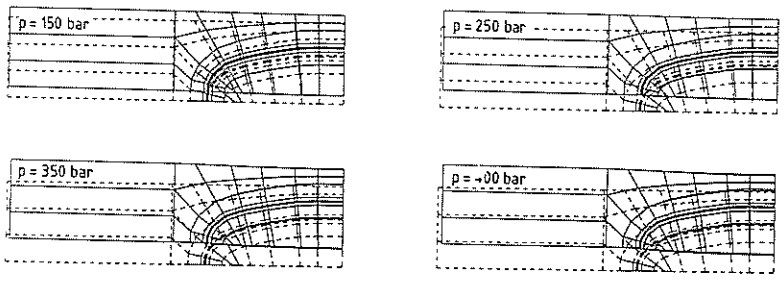

Fig. 8 - Displacement plots of the structure in the crack plane, plane, scaling factor 50

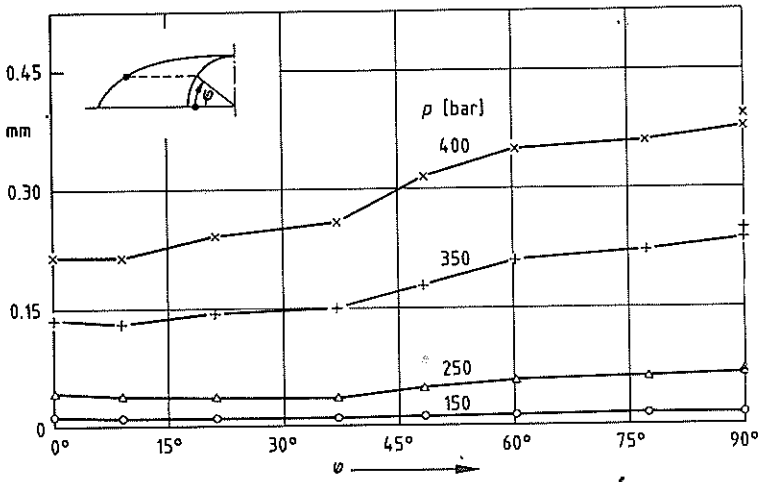

Fig. 9 - Crack tip opening displacement δ_t along the crack front for 150, 250, 350 and 400 bar

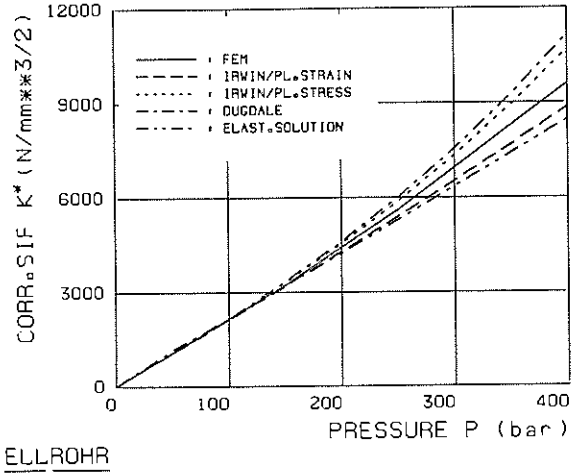

Fig. 11 - Comparison of several analytical approaches of the stress intensity factor K* for small scale yielding with results of FE-calculations

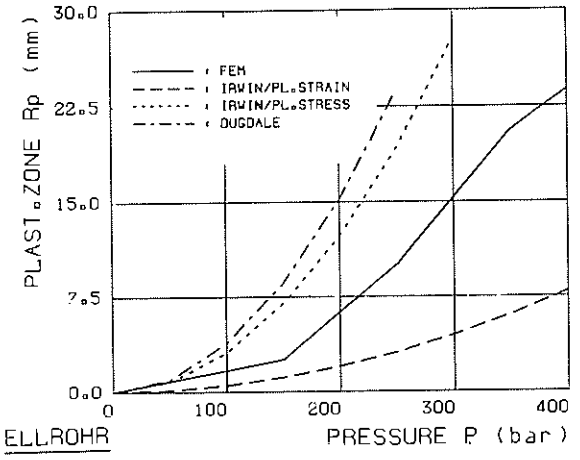

Fig. 10 - Radius of the plastic zone in dependence on pressure from FE-calculations and several small scale yielding approaches

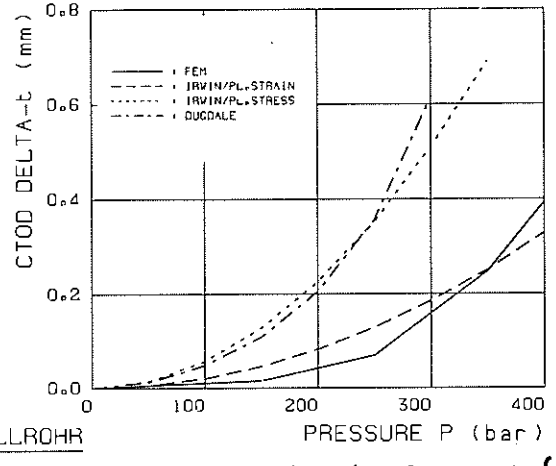

Fig. 12 - Crack tip opening displacement δ_t from FE-calculations in comparison with results of several analytical approaches